



AMS measurement of ^{10}Be concentrations in marine sediments from Chile Trench at the TANDAR laboratory



D. Rodrigues^{a,b,*}, A. Arazi^{a,b}, J.O. Fernández Niello^{a,b,c}, G.V. Martí^a, A.E. Negri^{b,c}, D. Abriola^a, O.A. Capurro^a, M.A. Cardona^{a,b,d}, E. de Barbará^a, F. Gollan^{a,b}, D. Hojman^{a,b}, A.J. Pacheco^{a,b}, N. Samsolo^a, M. Togneri^a, D. Villanueva^a

^a Departamento de Física Experimental, Laboratorio TANDAR, GlyA, Comisión Nacional de Energía Atómica, Av. Gral. Paz 1499, B1650KNA San Martín, Argentina

^b CONICET, Av. Rivadavia 1917, C1033AAJ Buenos Aires, Argentina

^c Instituto de Investigación e Ingeniería Ambiental, Universidad Nacional de San Martín, 25 de Mayo y Francia, B1650BWA San Martín, Buenos Aires, Argentina

^d Escuela de Ciencia y Tecnología, Universidad Nacional de San Martín, 25 de Mayo y Francia, B1650BWA San Martín, Buenos Aires, Argentina

ARTICLE INFO

Article history:

Received 12 November 2016

Received in revised form 3 January 2017

Accepted 18 January 2017

Keywords:

AMS

^{10}Be

Cosmogenic radionuclide

Marine sediments

ABSTRACT

The $^{10}\text{Be}/^9\text{Be}$ ratios in marine sediments samples from the Southern Chile Trench have been measured using accelerator mass spectrometry (AMS). The samples were measured at the TANDAR accelerator, where the discrimination of the ^{10}Be radionuclides was achieved by means of a passive absorber in front of an ionization chamber. This setup along with the high voltage available, provided a complete suppression of the ^{10}B isobar interference. The obtained values for the ^{10}Be concentrations, of the order of 10^9 - atoms/g, are the first ^{10}Be measurements from the Southern Chile Trench and offer an excellent tracer to quantitatively study the recycling of sediments in Andean magmas.

© 2017 Elsevier B.V. All rights reserved.

1. Introduction

In the last decades, accelerator mass spectrometry (AMS) has proven to be the most sensitive technique for detecting several long-lived radionuclides [1], ^{10}Be among them. This is the longest-lived beryllium radionuclide with a half-life of $(1.387 \pm 0.012) \times 10^6$ yr [2], primarily produced in Earth's atmosphere by cosmic-ray induced nuclear reactions on N and O [3]. Detectable amounts of ^{10}Be are present in rainwater, snow, surface water, and also in marine sediments [4]. It is an ideal radionuclide to be used as tracer in various branches of geosciences [5,6], as well as in astrophysics [7].

Small accelerators exclusively designed for AMS technique offer high transmission and stability. However, the higher beam energies achievable with large tandem accelerators allow the use of a passive absorber to efficiently suppress the interfering isobar (^{10}B in this case) and also get a better identification of other interfering ions with a telescope detector.

This manuscript reports the measurement at the 20 UD TANDAR (TANDem ARGentino) accelerator of the ^{10}Be concentration in two marine sediments samples from the Ocean Drilling Program (ODP) Site 860 [8]. This site is located at the so-called Chile Triple Junction, where Nazca, Antarctic and South American tectonic plates meet. The bulk of each sample was processed with the aim of quantifying the inventory of total ^{10}Be in the sediment. This is crucial to estimate the amount of sediment involved in the recycling process produced by the subduction of the oceanic plate underneath the South American Plate [9,10].

In Section 2 we describe the instrumentation used to carry out the AMS measurements. The chemical procedure performed, as well as the AMS measurement procedure are described in Section 3. In Section 4 we present the results and discussion and the conclusions in Section 5.

2. Instrumentation

As part of the AMS program at the TANDAR Laboratory [11,12] several improvements on the machine were carried out during the last years. A new Source of Negative Ions by Cesium Sputtering (SNICS II) was emplaced, the alignment of the experimental lines was carefully checked, the stability of the Generating Volt Meter

* Corresponding author at: Departamento de Física Experimental, Laboratorio TANDAR, GlyA, Comisión Nacional de Energía Atómica, Av. Gral. Paz 1499, B1650KNA San Martín, Argentina.

E-mail address: darodrig@tandar.cnea.gov.ar (D. Rodrigues).

(GVM) system was enhanced and the installation of a Wien filter is currently underway.

For AMS measurements, the switching between ^{10}Be and ^9Be beams was done changing the terminal voltage while keeping the magnetic rigidity at the high energy side fixed. In contrast to most of the facilities used for AMS, the TANDAR accelerator has two electrostatic quadrupoles and one electrostatic steerer along its 33-meters long acceleration column. These optical elements must be also adjusted according to the particle energy during switching between the radionuclide and its stable isotope. In fact, the proper tuning of the electrostatic steerer –placed just after the stripper– was of great importance in order to reduce scattered ions (see Section 3.3).

The main challenges in identifying ^{10}Be are dealing with molecular ($^9\text{Be}^1\text{H}$) and atomic (^{10}B) interfering isobars. The molecular ions get dissociated at the foil stripper at the terminal of the accelerator. The ^{10}B ions having the same electric charge state as the one selected for ^{10}Be after the foil stripper (3^+) cannot be differentiated by magnetic or electric deflectors. However, the high particle energy available by means of the TANDAR accelerator along with the use of a passive absorber in front of a ΔE -E telescope detector, allow discriminating ^{10}Be radionuclides from its stable isotope (those which manage to pass the analyzing magnet) and from other reaction products (see discussion below) with the complete suppression of ^{10}B .

Fig. 1 shows a scheme of the detection system built for ^{10}Be measurements. The passive absorber is a 150 mm long cylinder with a 17 mm diameter, 4 μm thick Havar[®] entrance window, based on a similar system developed at the Australian National University (ANU) in Canberra [13,14]. The absorber gas and the one used in the ionization chamber were kept separated by a 2 μm thick Havar[®] foil. Thus, choosing the appropriate Ar gas pressure in the passive absorber, the ^{10}B ions lose all their energy in the absorber, while the more penetrating ^{10}Be ions enter the ΔE -E telescope detector. This detector comprises an ionization chamber 110 mm long filled with 45 Torr P-10 gas followed by a surface barrier detector.

Absorber gas and window material were chosen in order to ensure the minimum content of hydrogen in them [14]. Otherwise, reactions products from the $^{10}\text{B} + ^1\text{H}$ interaction, namely ^7Be and ^4He ions, could reach the ΔE -E telescope detector and contribute to the background [15].

The optimal pressure within the passive absorber is the minimum necessary to completely stop the ^{10}B ions. This minimizes the energy loss and energy straggling for the ^{10}Be ions which arrive at the ionization chamber, and thus optimizing their identification. Energy loss calculations using the SRIM code [16] show that in a 150 mm long passive absorber with Ar gas, a pressure of 175 Torr –plus the 4- μm -Havar[®] window– is sufficient to stop ^{10}B ions having an energy of 27 MeV. Under these conditions the desired ^{10}Be ions arrive to the ionization chamber with enough

energy (about 11 MeV) to pass through the P-10 gas. Finally, these radionuclides reach the surface barrier detector placed behind the ionization chamber with an energy of about 8.5 MeV.

3. Experimental procedure

3.1. Production and standardization of ^{10}Be enriched material

The transmission of the system was studied by using commercial BeO powder enriched in ^{10}Be by neutron activation. This was achieved by irradiating the material with a thermal neutron flux of $\Phi = (6.1 \pm 0.3) \times 10^{13} \text{ cm}^{-2} \text{ s}^{-1}$ during (60 ± 1) min in the RA-3 reactor at the Ezeiza Atomic Center (Argentina) and producing ^{10}Be through the neutron capture reaction $^9\text{Be}(n, \gamma)^{10}\text{Be}$.

Both, enriched in ^{10}Be and non-irradiated powders were dissolved. Beryllium concentrations were calculated from the mass of BeO dissolved in both solutions and confirmed using Inductively Coupled Plasma Optical Emission Spectroscopy (ICP-OES) analysis, yielding compatible results within its relative error of 5 %.

Isotopically diluted material (nominal $^{10}\text{Be}/^9\text{Be} = (2.2 \pm 0.2) \times 10^{-11}$) from the enriched one was measured at ANU in Canberra [14], yielding $^{10}\text{Be}/^9\text{Be} = (2.10 \pm 0.06) \times 10^{-11}$. In this way, we standardize the enriched powder with a ratio of $^{10}\text{Be}/^9\text{Be} = (1.87 \pm 0.13) \times 10^{-9}$ traceable to the NIST standard material which was used at ANU.

Mixing in appropriate proportions the solutions of neutron-activated material and the commercial one (our “blank” material henceforth), six different ^{10}Be solutions with isotope ratios between $(9.2 \pm 0.8) \times 10^{-15}$ (blank only, see Section 3.2) and $(1.87 \pm 0.13) \times 10^{-9}$ (pure neutron-activated material) were prepared. Their corresponding isotope ratios were determined with a relative uncertainty of 6 %. The main contributions to the uncertainty come from the measurements of the concentrations and the determination of the volumes used in the mixtures.

3.2. Geological samples

The studied samples were taken from the Core 141-860B, Site 860 (ODP), located at the middle continental slope of the South American plate in the South Pacific Ocean ($45^\circ 51.972' \text{ S}$, $75^\circ 45.101' \text{ W}$). They correspond to depths of 0.77 mbsf (meter below sea floor, sample 001H) and 2.12 mbsf (sample 002H). The total beryllium content in both sediment samples was also determined by ICP-OES analyses. For chemical processing, 0.67 mg of beryllium carrier material was added to 300 mg of each sample. The isotope ratio of this carrier material had been previously measured at the Vienna Environmental Research Accelerator (VERA) [17], yielding $^{10}\text{Be}/^9\text{Be} = (9.2 \pm 0.8) \times 10^{-15}$.

The chemical separation of Be was performed according to the technique reported by Merchel and Herpers [18]. Hydroxides are

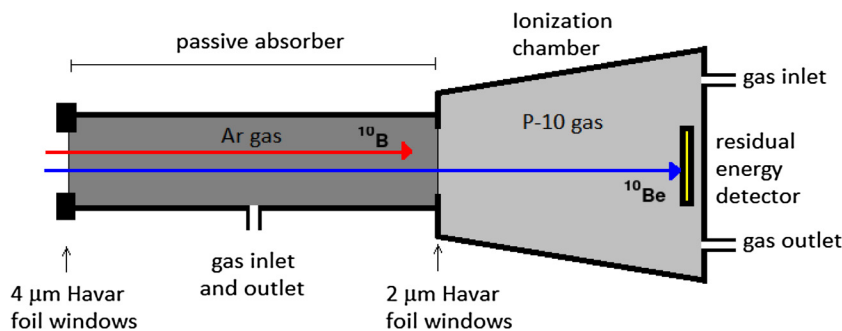


Fig. 1. Scheme of the passive absorber and the ΔE -E telescope detector used for the identification of ^{10}Be .

precipitated by addition of $\text{NH}_{3\text{aq}}$ and then Be is separated from the other elements by using anion and cation exchange columns. At the end of this process, $\text{NH}_{3\text{aq}}$ was added to the concentrated fraction eluted from the column and the beryllium hydroxide was obtained by precipitation. Finally, the hydroxide was washed and converted to beryllium oxide at 900 °C. This material was mixed with Ag powder (1:2 by weight) and pressed into Al sample holders of the ion source.

3.3. AMS measurements

^9Be and ^{10}Be were extracted from the ion source as negative molecular ions (BeO^-) and subsequently selected by the 90° double-focusing injection magnet (radius = 30 cm, $\text{ME}/Z^2 = 12$ amu-MeV). The tuning of the accelerator parameters for mass $A = 10$ was done optimizing the current of a macroscopic ^{10}B beam extracted from a natural boron sample. The tandem accelerator, operating at a terminal voltage of 8 MV, dissociates beryllium oxide molecules in a carbon foil stripper and accelerates $^{10}\text{Be}^{3+}$ ions to 27 MeV particle energy. A second 90° double-focusing analyzing magnet (radius = 200 cm, $\text{ME}/Z^2 = 500$ amu-MeV) selects these ions, eliminating most of the ^9Be background.

One of the ^{10}Be enriched samples (with $^{10}\text{Be}/^9\text{Be} = (6.2 \pm 0.4) \times 10^{-11}$) was used as standard material to define the region of interest (RoI) for ^{10}Be in the two-dimensional spectra (residual energy vs. partial energy loss taken from the Si detector and the ionization chamber, respectively) as it is shown in Fig. 2. This standard was used to determine the beam transmission, measuring it for 5 min before and after each unknown sample. Typical measuring time for the samples was 30 min.

Although the passive absorber prevents ^{10}B ions from entering into the ΔE -E telescope detector, there is another source of background due to charge exchange collisions with the residual gas (pressure around 10^{-8} Torr) within the high-energy side of the accelerator. In this way, ^9Be ions (changing from charge state 4^+ to 3^+) may acquire the same magnetic rigidity than $^{10}\text{Be}^{3+}$ and be accepted by the analyzing magnet [19]. These ions have higher energy than ^{10}Be ions and hence are clearly distinguishable from the ^{10}Be through their higher residual energy in the surface barrier detector as well as through their lower partial energy loss into the ionization chamber. However, when ^9Be ions lose energy by scattering in the beam line after the analyzing magnet, they may produce background events in the two-dimensional spectrum close to the RoI defined for ^{10}Be . This effect was studied by increasing the ^9Be beam intensity favoring the entrance of ^9Be particles by fixing the injection magnet to mass 25, which corresponds to the $^9\text{Be}^{16}\text{O}^-$

molecular ions, but keeping the high energy side optimized for ^{10}Be . Then, the fraction of scattered ^9Be ions with respect to the total ^9Be ions was minimized adjusting optic elements inside the acceleration column, being the electrostatic steerer at the terminal the most relevant. The subsequent tuning of the injector magnet and of the terminal voltage using the ^{10}B beam did not affect this adjustment.

4. Experimental results

Fig. 2a shows the two-dimensional spectrum obtained by measuring standardized material with $^{10}\text{Be}/^9\text{Be} = (6.2 \pm 0.4) \times 10^{-11}$. As can be seen, ^{10}Be ions can be unambiguously identified and discriminated from ^9Be ions that underwent charge-exchange collisions with the residual gas. As expected, there is no events of ^{10}B nor of scattered ^9Be ions in the spectrum.

Using our blank material ($^{10}\text{Be}/^9\text{Be} = (9.2 \pm 0.8) \times 10^{-15}$), and having a transmission of about 20%, two runs of one hour each with a mean current of 15 (electrical) nA of ^9Be , were performed without any events in the region of interest (RoI) for ^{10}Be . Considering the uncertainties in the transmission and the current instability a conservative upper limit for the sensitivity of 5×10^{-13} can be set.

This limit is two orders of magnitude lower than the typical $^{10}\text{Be}/^9\text{Be}$ ratios in environmental samples [4], even after isotope dilution with carrier material.

The $^{10}\text{Be}/^9\text{Be}$ ratio in the two 001H and 002H marine samples was measured with this setup. The recorded spectrum for sample 002H is shown in Fig. 2b. A few events appear below the RoI for ^{10}Be . By means of SRIM code simulations, they have been identified as ^7Be originating from the $^{10}\text{B}(^1\text{H}, ^4\text{He})^7\text{Be}$ reaction. In fact, ^4He also appears on the left side of the spectrum.

The total ^{10}Be concentrations were determined from the corresponding measured $^{10}\text{Be}/^9\text{Be}$ ratios (which include carrier material), considering the measured beryllium concentrations, the mass processed, and the added carrier for each sample. Table 1 summarizes the results of this work, where total intrinsic $^{10}\text{Be}/^9\text{Be}$ ratio correspond to the sediment (without carrier material). The ^{10}Be concentration of the samples 001H and 002H resulted $(2.7 \pm 0.8) \times 10^9$ atoms/g and $(1.4 \pm 0.4) \times 10^9$ atoms/g, respectively.

Since the difference in depth for these samples is 1.35 m and the sedimentation rate for this core was determined to be 50 m/Ma [8], its ages should differ by less than 27 kyr, a negligible time interval in comparison with the ^{10}Be half-life. Therefore, the ^{10}Be concentrations are not expected to have significant differences due to their difference in depth. However, in sediments close to a conver-

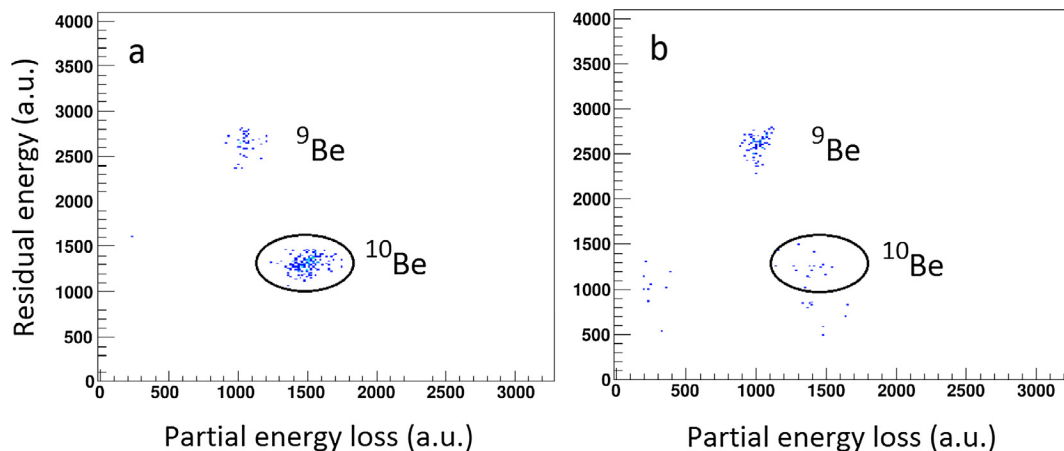


Fig. 2. Two-dimensional spectra recorded with the ΔE -E telescope detector. Panel a: standardized material with $^{10}\text{Be}/^9\text{Be} = (6.2 \pm 0.4) \times 10^{-11}$. Panel b: marine sediment sample 002H with $^{10}\text{Be}/^9\text{Be} = (1.0 \pm 0.3) \times 10^{-11}$. In the latter, the products of the reaction between ^{10}B and ^1H , i.e. ^4He and ^7Be , can also be identified.

Table 1

It shows the Be concentrations, the measured ratios of $^{10}\text{Be}/^9\text{Be}$ and the corresponding intrinsic ratio, and the total ^{10}Be concentrations (in the bulk) of marine sediment samples at ODP site 860.

Sample	001H	002H
Depth (mbsf)	0.77 ± 0.04	2.12 ± 0.04
Total beryllium concentration (ppm)	1.51 ± 0.08	1.48 ± 0.07
Total $^{10}\text{Be}/^9\text{Be}$ measured	$(1.8 \pm 0.5) \times 10^{-11}$	$(1.0 \pm 0.3) \times 10^{-11}$
Total $^{10}\text{Be}/^9\text{Be}$ intrinsic	$(2.6 \pm 0.7) \times 10^{-9}$	$(1.5 \pm 0.4) \times 10^{-9}$
Total ^{10}Be concentration (atoms/g)	$(2.7 \pm 0.8) \times 10^9$	$(1.4 \pm 0.4) \times 10^9$

gent plate boundary there are other mechanisms, as turbidite-induced sediment reworking and deformation by thrust faulting, able to produce strong modifications in the ^{10}Be concentration depth profile [20]. The difference in ^{10}Be concentrations of both samples observed here is not large enough to demonstrate the occurrence of these phenomena.

^{10}Be concentration values determined in this work for the Chilean Trench are slightly below the ones reported in the works from Raisbeck et al. [21] and Brown [22], where the concentration value for pelagic marine sediment samples was between 3 and 7×10^9 atoms/g. Those values correspond to sediments from the open ocean, where the sedimentation rate is lower than the ones from converging margin close to the continent. Correspondingly, the ^{10}Be concentrations in pelagic marine sediment are expected to be higher.

The ^{10}Be concentrations from Chile margin studied in this work are in agreement with the ones found in marine sediments from Kurile Convergent Margin in Russia [9] where the total ^{10}Be concentrations are around of 3×10^9 atoms/g. In addition, they are also comparable with the reported by Bourles et al. [23] for 17 surface sediment samples from different ocean basins (between 0.3 and 6×10^9 atoms/g).

5. Summary and conclusions

Measurements of the isotope ratios $^{10}\text{Be}/^9\text{Be}$ at the TANDAR laboratory have demonstrated the feasibility of this facility for AMS measurements of ^{10}Be . To facilitate this goal, we implemented a detection system consisting of a passive absorber to completely suppress the presence of the isobaric interference of ^{10}B and a ΔE -E telescope detector for the ^{10}Be identification. Blank material having an isotope ratio of $^{10}\text{Be}/^9\text{Be} = 9 \times 10^{-15}$ has enabled the determination of the current sensitivity level of this accelerator as better than $^{10}\text{Be}/^9\text{Be} = 5 \times 10^{-13}$. With the improvements of the beam transmission that are currently being implemented and the commissioning of a Wien velocity filter which will efficiently suppress charge-exchange and scattered ^9Be ions it is expected to achieve much lower isotope ratios.

The isotope ratios measured in the marine sediments samples from ODP site 860 represent the first determination of a ^{10}Be inventory at the Southern Chile Trench. This is relevant for the use of ^{10}Be tracer in studying the sediment recycling in arc magmas of the Southern Andes. In most cases, even considering the isotope dilution due to addition of carrier, $^{10}\text{Be}/^9\text{Be}$ ratios in surface marine sediments and others environmental samples are found two orders of magnitude above the achieved sensitivity at TANDAR accelerator. This opens the possibility to conduct such kind of research at this facility.

Acknowledgments

We thank A. Wallner from the Australian National University for the measurement of the $^{10}\text{Be}/^9\text{Be}$ ratio in our standard material

and P. Steier from VERA for the measurement of the $^{10}\text{Be}/^9\text{Be}$ ratio in our blank material. We also thank to Raúl Jimenez for the ICP-OES measurements and to the RA-3 staff for the BeO irradiation. We are especially grateful with the Ocean Drilling Program for providing the marine sediment samples studied in this work. DR has been provided a doctoral fellowship from CONICET.

References

- [1] W. Kutschera, Applications of accelerator mass spectrometry, *Int. J. Mass Spectr.* 349–350 (2013) 203–218.
- [2] G. Korschinek, A. Bergmaier, T. Faestermann, U.C. Gerstmann, K. Knie, G. Rugel, A. Wallner, I. Dillmann, G. Dollinger, C.L. von Gostomski, K. Kossert, M. Maiti, M. Poutivtsev, A. Rimmert, A new value for the half-life of ^{10}Be by Heavy-Ion Elastic Recoil Detection and liquid scintillation counting, *Nucl. Instrum. Methods B* 268 (2010) 187–191.
- [3] J. Masarik, J. Beer, An updated simulation of particle fluxes and cosmogenic nuclide production in the Earth's atmosphere, *J. Geophys. Res. Atmos.* 114 (2009) 11103.
- [4] L.R. McHargue, P.E. Damon, The global beryllium 10 cycle, *Rev. Geophys.* 29 (1991) 141–158.
- [5] J.D. Morris, Applications of ^{10}Be to problems in the earth sciences, *Ann. Rev. Earth Planet Sci.* 19 (1991) 313.
- [6] J.K. Willenbring, F. von Blanckenburg, Meteoric cosmogenic Beryllium-10 adsorbed to river sediment and soil: applications for Earth-surface dynamics, *Earth Sci. Rev.* 98 (2010) 105–122.
- [7] J. Beer, K. McCracken, R. von Steiger, *Cosmogenic Radionuclides: Theory and Applications in the Terrestrial and Space Environments*, Physics of Earth and Space Environments, Springer-Verlag, Berlin Heidelberg, 2012, ISBN 978-3-642-14650-3.
- [8] J.H. Behrmann, S.D. Lewis, R. Musgrave, Site 860 – shipboard scientific party, *Proceedings of the Ocean Drilling Program, Initial Reports vol. 141* (1992) 159–238.
- [9] B.M. Dreyer, J.D. Morris, J.B. Gill, Incorporation of subducted slab-derived sediment and fluid in arc magmas: B-Be- ^{10}Be - ϵNd systematics of the Kurile convergent margin, Russia, *J. Petrol.* 51 (2010) 1761–1782.
- [10] C.R. Stern, Subduction erosion: rates, mechanisms, and its role in arc magmatism and the evolution of the continental crust and mantle, *Gondwana Res.* 20 (2011) 284–308.
- [11] D.E. Alvarez, J.O. Fernández Niello, M. di Tada, A.M.J. Ferrero, G.V. Martí, O.A. Capurro, A.J. Pacheco, J.E. Testoni, D. Abriola, A. Etchegoyen, E. Achterberg, M. Ramirez, The AMS program at the TANDAR accelerator, *Nucl. Instrum. Methods B* 123 (1997) 39–42.
- [12] J.O. Fernández Niello, R.G. Liberman, O.A. Capurro, A.M.J. Ferrero, G.V. Martí, A. J. Pacheco, D. Abriola, M. Ramirez, J.E. Testoni, E. Achterberg, D.E. Alvarez, M. di Tada, The AMS system and research program at the TANDAR laboratory, *Nucl. Instrum. Methods B* 172 (2000) 91–94.
- [13] L.K. Fifield, T.R. Ophel, G.L. Allan, J.R. Bird, R.F. Davie, Accelerator mass spectrometry at the Australian National University's 14UD accelerator: experience and developments, *Nucl. Instrum. Methods B* 52 (1990) 233–237.
- [14] L.K. Fifield, S.G. Tims, T. Fujioka, W.T. Hoo, S.E. Everett, Accelerator mass spectrometry with the 14UD accelerator at the Australian National University, *Nucl. Instrum. Methods B* 268 (2010) 858–862.
- [15] J. Klein, R. Middleton, H. Tang, Modifications of an FN tandem for quantitative ^{10}Be measurement, *Nucl. Instrum. Methods Phys. Res.* 193 (1982) 601–616.
- [16] J.F. Ziegler, M.D. Ziegler, J.P. Biersack, SRIM – the stopping and range of ions in matter, *Nucl. Instrum. Methods B* 268 (2010) 1818–1823.
- [17] P. Steier, R. Golser, W. Kutschera, A. Priller, C. Vockenhuber, S. Winkler, VERA, an AMS facility for all isotopes, *Nucl. Instrum. Methods B* 223 (2004) 67–71.
- [18] S. Merchel, U. Herpers, An update on radiochemical separation techniques for the determination of long-lived radionuclides via accelerator mass spectrometry, *Radiochim. Acta* 84 (1999) 215–219.
- [19] J.O. Fernández Niello, A. Arazi, O.A. Capurro, D. Abriola, A.M.J. Ferrero, L. Gladkiss, R.G. Liberman, G.V. Martí, A.J. Pacheco, M. Ramirez, J.E. Testoni, Spurious ionic charge states in a tandem accelerator, *Nucl. Instrum. Methods B* 223 (2004) 242–246.
- [20] D. Rodrigues, S. Merchel, G. Rugel, A. Arazi, J. H. Behrmann, J. O. Fernandez Niello, G. Korschinek, G. V. Martí. Authigenic $^{10}\text{Be}/^9\text{Be}$ and $^{26}\text{Al}/^{27}\text{Al}$ depth profiles in marine sediments as a record of turbidity currents and thrust faulting: a case study from the Southern Chile convergent plate margin (Submitted for publication).
- [21] G.M. Raisbeck, F. You, M. Lieuvin, J.C. Ravel, M. Fruneau, J.M. Loiseaux, ^{10}Be in the environment: some recent results and their applications, *Proc. Symp. Accel. Mass Spectrom.*, 1981, pp. 228–243.
- [22] L. Brown, Applications of accelerator mass spectrometry, *Ann. Rev. Earth Planet Sci.* 12 (1984) 39–59.
- [23] D. Bourles, G.M. Raisbeck, F. You, ^{10}Be and ^9Be in marine sediments and their potential for dating, *Geochim. Cosmochim. Acta* 53 (1989) 443–452.